EPR of Mn^{2+} in $Fe(NH_4)_2(SO_4)_2\cdot 6H_2O$, $Zn(NH_4)_2(SO_4)_2\cdot 6H_2O$, and $Mg(NH_4)_2(SO_4)_2\cdot 6H_2O$: Mn^{2+}-Fe^{2+} exchange interaction

Sushil K. Misra and Stefan Z. Korczak*
Physics Department, Concordia University, 1455 de Maisonneuve Boulevard West, Montreal, Canada H3G 1M8
(Received 20 March 1986)

X-band EPR measurements on Mn^{2+}-doped single isostructural crystals of three Tutton salts $M(NH_4)_2(SO_4)_2\cdot 6H_2O$, M = Fe, Zn, and Mg, have been made at room, liquid-nitrogen, and liquid-helium temperatures. A least-squares fitting method, employing numerical diagonalization of the spin Hamiltonian matrix, fitting simultaneously a large number of resonant field line positions, has been adopted to accurately evaluate the spin Hamiltonian parameters. The intensities of lines at liquid-helium temperature have been used to determine the absolute signs of parameters. From the known shape of the paramagnetic sample (M = Fe), the Mn^{2+}-Fe^{2+} exchange interaction has been estimated to be 3.75 GHz in the paramagnetic host $Fe(NH_4)_2(SO_4)_2\cdot 6H_2O$, using the g shift in the paramagnetic from that in the diamagnetic hosts (M = Zn, Mg).

I. INTRODUCTION

Room-temperature *X*-band EPR measurements on the (Mn^{2+}-doped) iron ammonium Tutton salt $Fe(NH_4)_2(SO_4)_2\cdot 6H_2O$ (FASH) have been previously reported by Janakiraman and Upreti.[1] They evaluated the values of the parameters from the resonant line positions obtained only for the magnetic field orientation along the Z principal axis of the b_2^m tensor, using perturbation expressions. The absolute signs of the parameters could not be unequivocally determined, both because they did not record spectra at liquid-helium temperature, and because their measurements were confined to only one orientation of the magnetic field. For example, they deduced opposite signs for the hyperfine parameters A and B. They reported the observation of EPR spectra corresponding to two physically inequivalent, but magnetically equivalent, Mn^{2+} sites in the unit cell, the corresponding principal Z axes making an angle of $70\pm 5°$ from each other. As for low-temperature measurements, they only reported that, at 77 K, the spectra did not change significantly from those observed at room temperature, the total spread of lines increasing slightly at 77 K. As for the Mn^{2+}-doped zinc ammonium Tutton salt $Zn(NH_4)_2(SO_4)_2\cdot 6H_2O$ (ZASH) and the magnesium ammonium Tutton salt $Mg(NH_4)_2(SO_4)_2\cdot 6H_2O$ (MASH), several studies have been reported in the literature. Abe and Koga[2,3] reported EPR measurements on Mn^{2+}-doped ZASH at temperatures below 1 K; in particular, the absolute sign of b_2^0 was found to be positive. Mn^{2+}-doped ZASH and MASH EPR studies were first reported by Bleaney and Ingram,[4] who carried out their measurements down to 20 K. They estimated the values of the parameters; the absolute signs of the fine-structure parameters were determined from the trend of the spread of the hyperfine sextets as a function of the external field intensity. In particular, the absolute sign of the parameter b_2^0 was determined to be positive. Hayashi and Ono[5] reported further Mn^{2+}-doped ZASH EPR studies at room temperature; their results were, however, in agreement with those reported by Bleany and Ingram.[4] Mn^{2+}-doped MASH was also studied at the Q band by Ingram.[6] He estimated the values of the parameters for Mn^{2+} in MASH. He noticed a slight reduction of the electronic splitting in MASH as compared to that in ZASH. Strach and Bramley[7] have recently reported their zero-field EPR results on Mn^{2+}-doped ZASH and MASH. Their motivation was to determine accurate values of the spin Hamiltonian parameters, as well as to resolve the ambiguity in the sign of b_2^0. Their measurements indicated a negative absolute sign of b_2^0 while Bleaney and Ingram[4] determined the positive sign for the same. (The sign of b_2^0 as found in Refs. 2, 3, 4, and that in Ref. 6 are apparently not in disagreement due to different choices of coordinate axes; see Sec. VI.)

In the presence of an external magnetic field, crystals containing paramagnetic ions become magnetized at liquid-helium temperatures. This is equivalent to the presence of an additional magnetic field inside the crystal, over and above the external field. This manifests itself as a shift of the g value in the paramagnetic host crystal from that in an isostructural diamagnetic host crystal, and depends on the shape of the crystal. Kittel[8] has shown that the g shift is $3M(4\pi/3-N_Z)/2H_0$, where N_Z is the demagnetization factor along the axis of symmetry, M is the magnetization, and H_0 is the external magnetic field intensity. In particular, $N_Z=4\pi/3$ for a spherical sample, while $N_Z=0$ for a thin disc when the magnetic-field direction is in the plane of the flat face of the disc. In addition to the shift due to the magnetization of the sample, there is another g shift experienced by paramagnetic ions when introduced into the host lattice of other paramagnetic ions. This is caused by the magnetic field produced by the host paramagnetic ions at the site of the guest paramagnetic ion whose EPR is being observed. This g shift, obviously, depends on the guest-host exchange interaction, as discussed in Sec. III below.

It is the purpose of the present paper to report detailed EPR measurements on Mn^{2+}-doped single crystals of FASH, ZASH, and MASH. The EPR will be used to estimate the absolute signs of the parameters both from the

 ©1986 The American Physical Society

relative intensities of the lines at liquid-helium temperature, as well as from the spread of the fine-structure sextets as a function of the magnetic-field strength. The values of the parameters will be evaluated rigorously by the use of a recently developed least-squares fitting procedure especially adapted to electron-nuclear spin-coupled systems. The accurate values of the g factors will be used to estimate the Mn^{2+}-Fe^{2+} exchange interaction in the FASH host. This study is similar to that made to estimate the Mn^{2+}-Ni^{2+} exchange interaction[9-11] and the Gd^{3+}-Yb^{3+} exchange interaction[12] from the g shift in a paramagnetic host crystal from that in an isostructural diamagnetic crystal.

II. g SHIFT

A. Exchange interaction

At liquid-helium temperature the exchange interaction of the Mn^{2+} ion with the host Fe^{2+} ions results in the presence of an internal magnetic field at the Mn^{2+} site, since magnetic moments are induced on the paramagnetic host ions (Fe^{2+}) due to the polarization effect of the external magnetic field. This results in a shift of the resonant field value in the paramagnetic host, equivalent to the shift of the g factor in the paramagnetic host from that in an isostructural host lattice containing diamagnetic ions. This g shift can be estimated by taking into account the effect of the Mn^{2+}-Fe^{2+} exchange interaction in a perturbation calculation.

Considering the nearest-neighbor Fe^{2+} host ions only, the total spin Hamiltonian of a Mn^{2+}-Fe^{2+} pair can be expressed as:

$$\mathcal{H}_T=\mathcal{H}+\mathcal{H}'+\mathcal{H}_P\ , \tag{2.1}$$

where

$$\mathcal{H}=g\mu_B\mathbf{S}\cdot\mathbf{H}+B_2^0O_2^0+B_2^2O_2^2+B_4^0O_4^0+B_4^2O_4^2+B_4^4O_4^4\ , \tag{2.2}$$

is the spin Hamiltonian of the Mn^{2+} ion ($S=\frac{5}{2}$) (see Sec. III for more details);

$$\mathcal{H}'=g_1\mu_B\mathbf{S}_1\cdot\mathbf{H}+\beta_2^0O_2^0+\beta_2^2O_2^2+\beta_4^0O_4^0+\beta_4^2O_4^2+\beta_4^4O_4^4 \tag{2.3}$$

is the spin Hamiltonian of the Fe^{2+} ion ($S_1=2$), and

$$\mathcal{H}_P=J\mathbf{S}\cdot\mathbf{S}_1\ , \tag{2.4}$$

represents the Mn^{2+}-Fe^{2+} pair exchange interactions, J being the exchange interaction constant.

The unperturbed wave functions of the pair are of the form $\psi_1(M)\psi_2(M')$, where $M=\pm\frac{5}{2},\pm\frac{3}{2},\pm\frac{1}{2}$ (for the Mn^{2+} ion) and $M'=\pm2,\pm1,0$ (for the Fe^{2+} ion). Thus, there is a total of 30 basis functions yielding a (30×30)-dimensional matrix for the pair system. Choosing the Z axis to be along the external magnetic field and treating $\mathcal{H}+\mathcal{H}'$ as the unperturbed Hamiltonian and $\mathcal{H}_P$ as the perturbation, the following perturbed eigenvalues are obtained, after neglecting smaller zero-order terms,

$$E(\pm\tfrac{1}{2},0)=E^0(\pm\tfrac{1}{2},0)+E^2(\pm\tfrac{1}{2},0)\ , \tag{2.5}$$

where

$$E^0(\pm\tfrac{1}{2},0)=\pm g\mu_BH_Z/2-\tfrac{8}{3}b_2^0-2\beta_2^0\ , \tag{2.6}$$

and

$$E^2(\pm\tfrac{1}{2},0)=96J^2/[\mp(g-g_1)\mu_BH_Z-\beta_2^0]+108J^2/[\pm(g-g_1)\mu_BH_Z-\beta_2^0]\ . \tag{2.7}$$

In writing (2.7), the fact that there are two nearest neighbors in a Tutton salt (separated by the unit-cell vector c) has been taken into account. From the resonance condition (for the transition $\frac{1}{2},0\leftrightarrow-\frac{1}{2},0$), $h\nu=g_{\text{obs}}\mu_BH_Z$ one obtains from (2.5)

$$g_{\text{obs}}=g-48J^2(g-g_1)/(\beta_2^0)^2\ , \tag{2.8}$$

where b_2^0 has been neglected, since $b_2^0\ll\beta_2^0$. Thus, J can be estimated from a knowledge of g and g_1, which are, respectively, the g factors for Mn^{2+} in the isostructural diamagnetic host and that for Fe^{2+} in FASH. When the magnetic field is along the X axis, β_2^0 in Eq. (2.8) should be replaced by $(\beta_2^0)'$ where $(\beta_2^0)'$ is the transformed parameter in the system of axes where the X axis is the principal axis of the β_2^m tensor. Thus, in this coordinate system

$$|J|=\left|\frac{g_{XX}^d-g_{XX}^p}{48(g_{XX}^d-g_1)}\right|^{1/2}|(\beta_2^0)'|\ . \tag{2.9}$$

In Eq. (2.9) g_{XX}^p, g_{XX}^d, and g_1 are, respectively, the g factors as observed in the paramagnetic Tutton salt (FASH) for Mn^{2+}, in the isostructural diamagnetic Tutton salt (ZASH or MASH) for Mn^{2+}, and in FASH for Fe^{2+}, respectively. $(\beta_2^0)'=1.5(\beta_2^2-\beta_2^0)$, where β_2^0 and β_2^2 refer to the Fe^{2+} parameters in FASH in the coordinate system in which the Z axis is the principal axis of the β_2^m tensor.

B. Shape effect

As mentioned in the Introduction, at low temperatures there is an additional g shift introduced by the shape of the crystal over and above that caused by the exchange interaction. In the particular case reported in this paper, the paramagnetic FASH crystal was chosen to be in the shape of a thin disc, the flat face containing the X_1,X_2 axes (see Sec. V, Fig. 1). The magnetization along the X axis can then be expressed as (in emu):

$$M_X=H(\chi_1\cos\alpha+\chi_2\cos\beta+\chi_3\cos\gamma)d/A\ . \tag{2.10}$$

In Eq. (2.10), χ_1,χ_2,χ_3 are the principal values of the susceptibility tensor, α,β,γ are the angles made by the principal directions of the susceptibility tensor with the X axis; d is the density of the FASH crystal, A is its molecular weight, and H is the intensity of the magnetic field.

When the magnetic field is along the X axis, which lies in the flat face of a thin disk, the shift in the g factor due to the shape of the crystal (as a thin disc) can be expressed as

$$\Delta g_{XX}=2\pi M_X/H=2\pi(\chi_1\cos\alpha+\chi_2\cos\beta+\chi_3\cos\gamma)d/A\ . \quad (2.11)$$

In Eq. (2.11), a demagnetization factor of 0, appropriate to a thin disk has been used. Eq. (2.11), combined with Eq. (2.10), can then be used to correct for the shape-dependent shift of the g factor.

III. SAMPLE PREPARATION, CRYSTAL STRUCTURE AND SPIN HAMILTONIAN

The crystals were grown by slow evaporation at room temperature of aqueous solutions of appropriate Tutton salts to which sufficient manganese sulfate had been added so as to introduce one Mn^{2+} ion for every 1000 Fe^{2+}, Zn^{2+}, or Mg^{2+} ions in the respective solution. The crystal-growth habit of FASH single crystal is illustrated in Fig. 1. In particular, the FASH crystals grow with a large flat face and a small rectangular face at right angles to it. This rectangular face is coincident with the ac plane. Similar growth habits are exhibited by ZASH and MASH crystals.

The crystal structure of Tutton salts is monoclinic (space group $P2_1/a$).[13] The unit cell parameters (a,b,c) are approximately in the ratio (3,4,2) while the angle β is about 105°. There are two formula units in the unit cell; the two physically inequivalent divalent cations are situated at points (0,0,0) and $(\frac{1}{2},\frac{1}{2},0)$, each being surrounded by a slightly distorted octahedron of water molecules. In particular, for FASH (Ref. 14) $a=9.32$ Å, $b=12.65$ Å, $c=6.24$ Å, $\beta=106.8°$; for ZASH (Ref. 15) $a=9.28$ Å, $b=12.57$ Å, $c=6.25$ Å, $\beta=106.8°$; and for MASH (Ref. 16) $a=9.38$ Å, $b=12.67$ Å, $c=6.22$ Å, $\beta=107.1°$.

The spin Hamiltonian applicable to EPR in Tutton salt is that appropriate to orthorhombic symmetry:[1,4,17]

$$\mathcal{H}=g_{ZZ}\mu_B H_Z S_Z+g_{XX}\mu_B H_X S_X+g_{YY}\mu_B H_Y S_Y+\sum_{m=0,2}\tfrac{1}{3}b_2^m O_2^m+\sum_{m=0,2,4}\tfrac{1}{60}b_4^m O_4^m+AS_ZI_Z+B(S_XI_X+S_YI_Y)+Q'[I_Z^2-\tfrac{1}{3}I(I+1)]+Q''[I_X^2-I_Y^2]\ . \quad (3.1)$$

In Eq. (3.1), g, μ_B, H, S $(=\frac{5}{2})$, I $(=\frac{5}{2})$, and O_l^m are, respectively, the g factor, Bohr magneton, magnetic field intensity, electronic spin (Mn^{2+} ion), nuclear spin (Mn^{2+} ion), and electron-spin operators (as defined by Bleaney and Abragam[18]). The X,Y,Z axes are defined to be coincident with the axes of the b_2^m tensor in such a way that the splittings of the $\Delta M=\pm1$ lines (M is the electronic quantum number) display extrema along X, Y, and Z; the maximum spread of these extrema is obtained for $\mathbf{H}||\hat{\mathbf{Z}}$ and minimum for $\mathbf{H}||\hat{\mathbf{Y}}$.[19] The orientations of these axes corresponding to the two physically inequivalent, but magnetically equivalent, sites for Mn^{2+} are illustrated in Fig. 1, which also exhibits the orientations of the magnetic susceptibility axes K_1,K_2,K_3.[20] (There is only one set of these axes.) In particular, it should be noted that $\mathbf{K}_3||\mathbf{b}$ (Fig. 1). The parameters Q' and Q'' cannot be determined from the positions of the "allowed" lines ($\Delta M=\pm1$, $\Delta m=0$; M and m are the electronic and nuclear spin quantum numbers), as the corresponding resonant magnetic fields do not depend upon Q' and Q''.

IV. EXPERIMENTAL ARRANGEMENT

A Varian V4506 X-band spectrometer was used for the investigations reported in this paper. The magnetic field was measured using a Burker Gaussmeter (B-NM20). The temperature of the sample was varied inside a liquid-nitrogen or liquid-helium cryostat containing a heater resistor. For angular variation studies at low temperatures, the magnetic field was rotated keeping the sample fixed, while at room temperature it was the crystal which was rotated keeping the direction of the magnetic field fixed.

V. DATA AND EVALUATION OF PARAMETERS

The features of the EPR spectra of Mn^{2+} in all three hosts, FASH, ZASH, and MASH, are the same. At any temperature, there are observed two sets of spectra typical of Mn^{2+} ions (a total of 30 allowed lines, i.e., five hyperfine sextets), corresponding to the two sites in the unit cell into which Mn^{2+} ions can substitute. Except for the

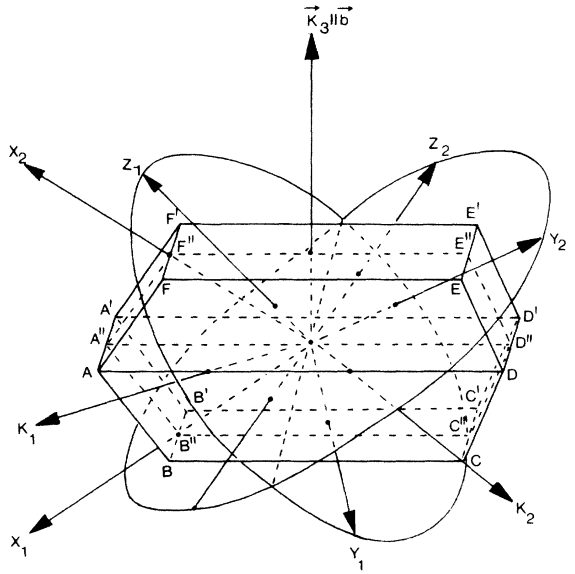

FIG. 1. Orientations of the EPR axes X_1,Y_1,Z_1; X_2,Y_2,Z_2; and the magnetic susceptibility axes K_1,K_2,K_3 in relation to the crystal-growth habit of a FASH host. *ABCDEF* represents the large flat face into which the crystal grows. *EE'F'F* is the small rectangular face of the crystal which is coincident with the *ac* plane; it is parallel to the K_1,K_2 plane. The plane *DD'A'A* is parallel to *EE'F'F*, while the plane *A''B''C''D''E''F''* is parallel to *ABCDEF*. The solid points drawn at the intersection of some lines indicate that those lines actually cross each other. It should be noted that the plane *ADD'A'* lies symmetrically with respect to the planes containing the Y_1,Z_1 and the Y_2,Z_2 axes. The angles α,β,γ made by K_1,K_2,K_3 with the X_1 axis are 59.7°, 49.8°, and 55°, respectively.

difference in the orientations of the X,Y,Z axes these two sets of spectra are identical in all respects. The angular variation of room-temperature spectra in the ZX plane of one site for FASH at liquid-helium temperature is displayed in Fig. 2. It is seen that at room temperature the overall separation of the lines for $\mathbf{H}||\hat{\mathbf{Z}}$ is only slightly greater than that for $\mathbf{H}||\hat{\mathbf{X}}$. As the temperature is lowered it is found for all three, FASH, ZASH, and MASH, samples that the overall separation of lines for $\mathbf{H}||\hat{\mathbf{X}}$ starts to increase, while that for $\mathbf{H}||\hat{\mathbf{Z}}$ remains almost the same. Ultimately, below about 240, 250, and 130 K this separation for $\mathbf{H}||\hat{\mathbf{X}}$ becomes greater than that for $\mathbf{H}||\hat{\mathbf{Z}}$ for FASH, ZASH, and MASH, respectively. This is exhibited for the FASH host in Fig. 3; similar patterns are obtained for FASH and MASH hosts. This means that as the temperature is lowered the magnitude of the parameter b_2^2 increases, finally becoming greater than that of b_2^0 at lower temperatures. (See Table I, listing the parameters.) This behavior is similar to that observed for Gd^{3+} in rare-earth-metal acetate tetrahydrates.[21]

As far as the orientations of the X,Y,Z axes, corresponding to the two inequivalent sites, are concerned, the following should be noted. When the magnetic field orientation is in the ac plane, there is observed only one set of spectra, indicating that this plane is the mirror plane reflecting the axes corresponding to one physically inequivalent ion into those corresponding to the other inequivalent ion. Thus, the two sites are oriented symmetrically to the ac plane. The two X axes lie in the flat plane $A''B''C''D''E''F''$ (Fig. 1), the angle between X_1 and X_2 being $70°\pm1°$ for FASH. The two Z axes for FASH are found to lie in the K_1K_3 plane at angles $\pm41.5°$ from the ac plane. The X_2 and Y_2 axes corresponding to the Z_2 axis (at $-41.5°$ from the ac plane) are found to make, respectively, the angles 35° and 30° with the ac plane (see Fig. 1). For the other site, the X_1, Y_1 axes, likewise, make angles of $-35°$ and $-30°$, respectively with the ac plane. No measurements of these angles were made for ZASH and MASH in the present investigations.

The spin Hamiltonian parameters were determined by the use of a recently developed least-squares fitting (LSF) procedure in which a large number of resonant line positions, observed for $\mathbf{H}$ in the ZX plane, are simultaneously fitted, and the 36×36 spin Hamiltonian matrix is numerically diagonalized on a digital computer.[22] The evaluation is done in two steps.[22] First, from the fine line positions deduced from hyperfine sextets, assuming that the hyperfine interaction is absent, the fine-structure parameters are evaluated. These values are then used as initial values in a subsequent LSF procedure to accurately evaluate all the spin Hamiltonian (SH) parameters (fine and hyperfine) fitting simultaneously all clearly discernible resonant line positions. This means that anywhere from 200 to 300 line positions are used. (This includes line positions obtained for magnetic field orientation between 0° and 24° and between 66° and 90° in the ZX plane for the three hosts.) This reduces the parameter errors considerably.[23]

The absolute signs of the parameters are obtained from the relative intensities of the lines at liquid-helium temperature. In the spectrum for $\mathbf{H}||\hat{\mathbf{Z}}$, as the temperature is lowered to the liquid-helium temperature, the intensity of the highest-field sextet decreases relative to that of the lowest-field sextet for all the three hosts—FASH, ZASH, and MASH. This indicates that the absolute sign of b_2^0 is negative for all three hosts.[18] It is also in accordance with the negative absolute sign for b_2^0 as indicated by the spread of the various sextets. This spread decreases as H increases for all the three hosts, indicating that the abso-

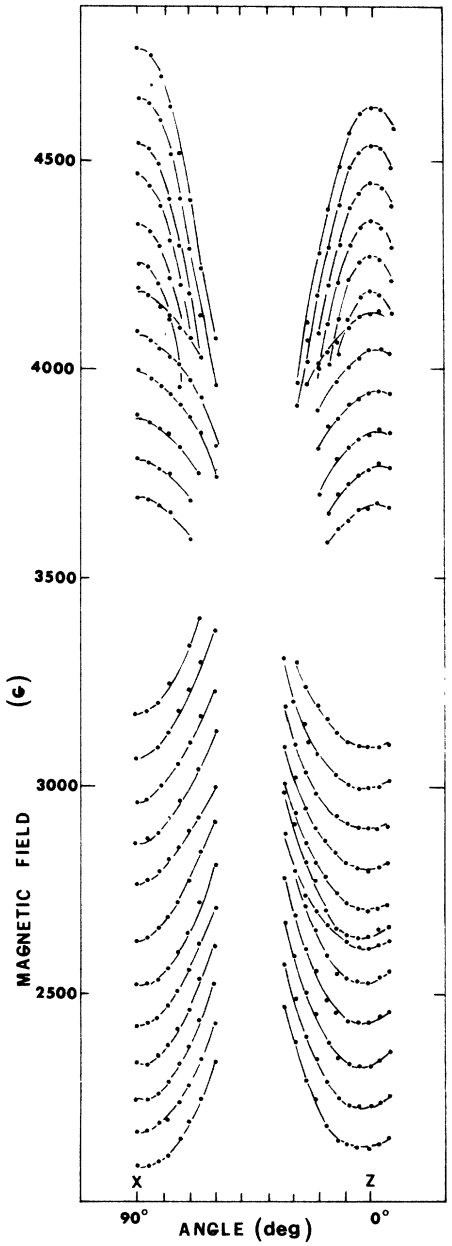

FIG. 2. Angular variation of X-band EPR spectra in the ZX plane for one of the physically inequivalent, but magnetically equivalent, sites for the FASH host at liquid-helium temperature (4.5 K). The circles represent the experimental resonant line positions, and the solid lines are smooth curves that connect data points from the same transition.

TABLE I. Values of the spin Hamiltonian parameters for the Mn^{2+}-doped ZASH host (0.1%). The parameters b_l^m, A, and B are expressed in units of GHz. The indicated errors are as estimated by the use of a statistical method (Ref. 23). The parameters reported by other workers have also been included for comparison. It should be noted that the Z and X axes chosen in Refs. 4 and 6 do not correspond to X and Z axes of the present work, which are the same as those of Refs. 1 and 7. (For more details see Sec. IV.) The values of b_4^0 and b_4^4 have been estimated from the values of the parameters a and F given the Refs. 4 and 6; specifically $b_4^0=(a+F)/2$, $b_4^4=2.5a$. RT stands for room temperature. n represents the number of lines simultaneously fitted.

Parameter	295 K[a]	293 K[b]	230 K[c]	RT[d]	85 K[a]	4.2 K[a]	20 K[c]
g_{zz}	2.007±0.001			2.000	2.007±0.001	2.003±0.001	1.998
g_{xx}	2.009±0.001				2.003±0.001	2.004±0.001	2.000
b_2^0	−0.710±0.002	−0.721	0.720	0.718	−0.726±0.001	−0.738±0.001	0.831
b_2^2	0.592±0.004	0.677	0.900	0.673	0.863±0.002	0.833±0.002	0.450
b_4^0	0.004±0.001	0.011			0.005±0.001	0.004±0.001	
b_4^2	−0.050±0.019	0.005			0.040±0.011	−0.042±0.008	
b_4^4	0.012±0.022	0.040	0.0375	0.034	0.102±0.011	0.028±0.010	0.060
A	−0.270±0.003	−0.264	−0.2733	−0.2735	−0.274±0.002	−0.276±0.017	−0.273
B	−0.270±0.004	−0.264			−0.257±0.002	−0.249±0.019	−0.283
n	234	31			264	267	

[a]This work.
[b]Strach and Bramley (Ref. 7) (B represents the average of A_X and A_Y).
[c]Bleaney and Ingram (Ref. 4).
[d]Hayashi and Ono (Ref. 5).

TABLE II. Values of the spin Hamiltonian parameters for the Mn^{2+}-doped FASH and MASH hosts (0.1% doping for each). For details and notation, see the caption of Table I.

Parameter	295 K[a]	RT[b] FASH	60 K[a]	4.5 K[a]	295 K[a]	293 K[c]	RT[d] MASH	29 K[a]	4.5 K[a]
g_{zz}	2.005±0.001	2.004	2.054±0.001	2.013±0.001	2.009±0.001			2.005±0.001	2.007±0.001
g_{xx}	1.989±0.001		1.994±0.001	1.983±0.001	2.007±0.001			2.003±0.001	2.005±0.001
b_2^0	−0.722±0.001	−0.698	−0.719±0.002	−0.727±0.001	−0.723±0.001	−0.723	0.693	−0.723±0.001	−0.731±0.001
b_2^2	0.557±0.004	0.405	0.865±0.004	0.824±0.002	0.470±0.002	0.566	0.540	0.811±0.002	0.803±0.002
b_4^0	0.004±0.001		0.002±0.001	0.009±0.001	0.009±0.001	0.007		0.002±0.001	0.004±0.001
b_4^2	−0.079±0.012		0.019±0.010	−0.051±0.009	0.053±0.007	0.0		−0.077±0.012	−0.007±0.016
b_4^4	0.119±0.002		0.062±0.017	0.161±0.009	0.004±0.008	0.036	0.023	−0.001±0.013	0.090±0.015
A	−0.276±0.002	−0.263	−0.275±0.002	−0.275±0.002	−0.261±0.002	−0.264	−0.270	−0.276±0.002	−0.281±0.002
B	−0.246±0.003	−0.272	−0.235±0.003	−0.251±0.002	−0.245±0.002	−0.266	−0.270	−0.249±0.002	−0.251±0.002
n	228		218	246	219	34		269	232

[a]This work.
[b]Janakiraman and Upreti (Ref. 1).
[c]Strach and Bramley (Ref. 7) (B represents the average of A_X and A_Y).
[d]Ingram (Ref. 6).

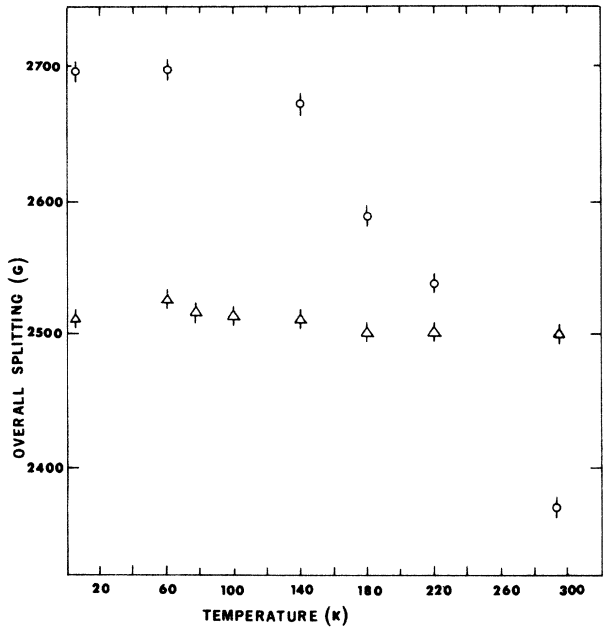

FIG. 3. Plot of the overall splitting of the EPR lines for the FASH host for $\mathbf{H}||\hat{\mathbf{X}}$ and for $\mathbf{H}||\hat{\mathbf{Z}}$ as a function of temperature. (Similar plots are obtained for ZASH and MASH hosts.) The circles represent points for $\mathbf{H}||\hat{\mathbf{X}}$, while the triangles represent points for $\mathbf{H}||\hat{\mathbf{Z}}$.

lute signs of b_2^0 and A are the same. Since the hyperfine interaction data yield a negative absolute sign for A,[24] b_2^0 also has a negative absolute sign. The relative signs of parameters are correctly determined by the LSF procedure. Thus, the absolute signs of all the parameters are determined unequivocally.

The average linewidth is the same (about 12 G) at all temperatures, for all orientations of the magnetic field and for all strengths of the magnetic field, for ZASH and MASH hosts. As for the FASH host, it is independent of the orientation or the strength of the magnetic field, being about 12 G between room and liquid-nitrogen temperature and about 18 G at liquid-helium temperature.

At liquid-helium temperature some extra lines at lower magnetic field are observed for FASH. These may be attributed to Fe^{2+} ion.[20,25]

The values of the SH parameters for Mn^{2+} in ZASH are recorded in Table I, which also contains the values reported previously by other researchers. The corresponding results for FASH and MASH are listed in Table II.

VI. DISCUSSION

The following points are worthy of discussion.

A. Ambiguity in the absolute sign of b_2^0

The absolute sign of b_2^0, as reported by Bleaney and Ingram[4] for Mn^{2+} in ZASH, is positive, while the present measurements indicate a negative absolute sign. These observations are, however, not contradictory. As Strach and Bramley[7] have noted, the Z and X axes chosen in Ref. 4 are, indeed, coincident with their X and Z axes, respectively. The X and Z axes, as defined in the present work (Sec. III), are found to be identical to those given in Ref. 7. This is further evidenced by the EPR spectra of Ref. 7 for $\mathbf{H}||\hat{\mathbf{Z}}$ and $\mathbf{H}||\hat{\mathbf{X}}$, being similar to those observed in the present investigation. Thus, if one were to transform the b_2^0, b_2^2 values as given in Table I of the present paper to new $(b_2^0)'$ and $(b_2^2)'$ values, where $Z \rightarrow X$ and $X \rightarrow Z$, one would, indeed, find a positive absolute sign for $(b_2^0)'$ $[=1.5(b_2^0 - b_2^0)]$.

B. Behavior of overall separation of lines for $\mathbf{H}||\hat{\mathbf{Z}}$ and $\mathbf{H}||\hat{\mathbf{X}}$

It is found that for all the three hosts, FASH, ZASH, and MASH, the overall separation of lines for $\mathbf{H}||\hat{\mathbf{Z}}$ is slightly greater than that for $\mathbf{H}||\hat{\mathbf{X}}$ at room temperature. However, this splitting for $\mathbf{H}||\hat{\mathbf{Z}}$ does not change significantly with temperature, while that for $\mathbf{H}||\hat{\mathbf{X}}$ increases substantially with decreasing temperature, finally surpassing the overall splitting for $\mathbf{H}||\hat{\mathbf{Z}}$ below certain temperatures for the three hosts. This behavior can be explained to be due to the relative change in the positions of the oxygen atoms and water molecules surrounding the Mn^{2+} ion, as the temperature is lowered. (Similar behavior was observed for the EPR of Gd^{3+} in rare-earth-metal acetate tetrahydrates.[21])

C. Orientations of X, Y, Z axes

Detailed measurements were made on the FASH host in the present report to determine the orientations of the X, Y, Z axes (as defined in Sec. III) with respect to the crystal planes. It was found that $\hat{\mathbf{X}}_1, \hat{\mathbf{Y}}_1, \hat{\mathbf{Z}}_1$ make angles of $-41.5°$, $35°$, and $-30°$, respectively, with the ac plane. The magnetic susceptibility axis $\mathbf{K}_3$ is parallel to the b axis.[20] For ZASH, Strach and Bramley[7] found that the X_1 and Z_1 axes make angles of $-33°$ and $33°$, respectively with the ac plane, while the X_2 and Z_2 axes make angles of $+33°$ and $-33°$, respectively with the ac plane. No detailed measurements have been reported for MASH.

D. Mn^{2+}-Fe^{2+} exchange interaction

Using the values given in Tables I and II, and the angles made by the susceptibility axes K_1, K_2, K_3 (Fig. 1) with the X_1 axis the Mn^{2+}-Fe^{2+} exchange interaction can be estimated. Specifically, for use in Eq. (2.9) for Fe^{2+} in FASH[20] $\beta_2^0 = 379.8$ GHz; g_{XX}^d is taken to be the average of g_{XX} values for ZASH and MASH hosts; as for g_{XX}^e, the g_{XX} value for the FASH host was used, suitably corrected for a shape-dependent factor using Eq. (2.11). For use in Eq. (2.11) $\chi_1 = 1.02$ emu/mol, $\chi_2 = 0.05$ emu/mol, $\chi_3 = 0.79$ emu/mol, $\alpha = 59.7°$, $\beta = 49.8°$, $\gamma = 55°$ as given in Ref. 20, and $d = 1.864$ g/cm^3, $A = 392.14$. Finally, the Mn^{2+}-Fe^{2+} exchange interaction constant is evaluated to be 3.75 GHz.

ACKNOWLEDGMENTS

The authors are grateful to the Natural Sciences and Engineering Research Council of Canada for financial support (Grant No. A4485), and to the Concordia University Computer Centre for computing facilities.

*Permanent address: Department of Experimental Physics, Maria Curie—Sklodowska University, 20-031 Lublin, Poland.

[1]R. Janakiraman and G. C. Upreti, Chem. Phys. Lett. **4**, 550 (1970).
[2]H. Abe and K. Koga, Phys. Rev. Lett. A **49**, 17 (1974).
[3]H. Abe and K. Koga, J. Phys. Soc. Jpn. **38**, 99 (1975).
[4]B. Bleaney and D. J. E. Ingram, Proc. R. Soc. London, Ser. A **205**, 336 (1951).
[5]I. Hayashi and K. Ono, J. Phys. Soc. Jpn. **8**, 270 (1953).
[6]D. J. E. Ingram, Proc. Phys. Soc. London A **66**, 412 (1953).
[7]S. J. Strach and R. Bramley, J. Magn. Reson. **56**, 10 (1984).
[8]C. Kittel, Phys. Rev. **73**, 155 (1948).
[9]S. K. Misra and M. Kahrizi, Phys. Rev. B **28**, 5300 (1983).
[10]S. K. Misra and M. Kahrizi, Phys. Rev. B **30**, 2920 (1984).
[11]S. K. Misra and M. Kahrizi, Phys. Rev. B **30**, 5352 (1984).
[12]S. K. Misra, M. Kahrizi, P. Mikolajczak, and L. Misiak, Phys. Rev. B **32**, 4738 (1985).
[13]W. Hoffman, Z. Kristallogr., Kristallogeom., Kristallphys., Kristallchem. **78**, 279 (1931); G. M. Brown and R. Chidambaram, Acta Crystallogr. Sect. B **25**, 676 (1969), and references therein.
[14]H. Montgomery, Acta Crystallogr. **22**, 775 (1967).
[15]H. Montgomery and E. C. Lingafelter, Acta Crystallogr. **17**, 1295 (1964).
[16]H. Montgomery and E. C. Lingafelter, Acta Crystallogr. **17**, 1478 (1964).
[17]V. K. Jain, Z. Naturforsch. Teil A **32**, 1364 (1977).
[18]B. Bleaney and A. Abragam, *Electron Paramagnetic Resonance of Transition Ions* (Clarendon, Oxford, 1970).
[19]M. Weger and W. Low, Phys. Rev. **111**, 1526 (1958).
[20]J. C. Gill and P. A. Ivey, J. Phys. C **7**, 1536 (1974).
[21]S. K. Misra, M. Bartkowski, and P. Mikolajczak, J. Chem. Phys. **78**, 5369 (1983).
[22]S. K. Misra, Physica **121B**, 193 (1983).
[23]S. K. Misra and S. Subramanian, J. Phys. C **15**, 7199 (1982).
[24]A. Steudel, *Hyperfine Interactions* (Academic, New York, 1976), p. 182.
[25]D. M. S. Bagguley, B. Bleaney, J. H. E. Griffiths, R. P. Penrose, and B. I. Plumpton, Proc. Phys. Soc. London **61**, 551 (1948).